Biology of Human Tumors

Clinical Cancer Research

Genomic Copy Number Profiling Using Circulating Free Tumor DNA Highlights Heterogeneity in Neuroblastoma

Mathieu Chicard[1,2], Sandrine Boyault[3], Leo Colmet Daage, [1,2], Wilfrid Richer[1,2], David Gentien[4], Gaelle Pierron[5], Eve Lapouble[5], Angela Bellini[1,2], Nathalie Clement[1,6], Isabelle Iacono[7], Stéphanie Bréjon[7], Marjorie Carrere[3], Cécile Reyes[4], Toby Hocking[8], Virginie Bernard[9], Michel Peuchmaur[10], Nadège Corradini[11], Cécile Faure-Conter[11], Carole Coze[12], Dominique Plantaz[13], Anne Sophie Defachelles[14], Estelle Thebaud[15], Marion Gambart[16], Frédéric Millot[17], Dominique Valteau-Couanet[18], Jean Michon[6], Alain Puisieux[19], Olivier Delattre[1,2,5,9], Valérie Combaret[7], and Gudrun Schleiermacher[1,2,6]

Abstract

Purpose: The tumor genomic copy number profile is of prognostic significance in neuroblastoma patients. We have studied the genomic copy number profile of cell-free DNA (cfDNA) and compared this with primary tumor arrayCGH (aCGH) at diagnosis.

Experimental Design: In 70 patients, cfDNA genomic copy number profiling was performed using the OncoScan platform. The profiles were classified according to the overall pattern, including numerical chromosome alterations (NCA), segmental chromosome alterations (SCA), and *MYCN* amplification (MNA).

Results: Interpretable and dynamic cfDNA profiles were obtained in 66 of 70 and 52 of 70 cases, respectively. An overall identical genomic profile between tumor aCGH and cfDNA was observed in 47 cases (3 NCAs, 22 SCAs, 22 MNAs). In one case, cfDNA showed an additional SCA not detected by tumor aCGH. In 4 of 8 cases with a silent tumor aCGH profile, cfDNA analysis revealed a dynamic profile (3 SCAs, 1 NCA). In 14 cases, cfDNA analysis did not reveal any copy number changes. A total of 378 breakpoints common to the primary tumor and cfDNA of any given patient were identified, 27 breakpoints were seen by tumor aCGH, and 54 breakpoints were seen in cfDNA only, including two cases with interstitial *IGFR1* gains and two alterations targeting *TERT*.

Conclusions: These results demonstrate the feasibility of cfDNA copy number profiling in neuroblastoma patients, with a concordance of the overall genomic profile in aCGH and cfDNA dynamic cases of 97% and a sensitivity of 77%, respectively. Furthermore, neuroblastoma heterogeneity is highlighted, suggesting that cfDNA might reflect genetic alterations of more aggressive cell clones. *Clin Cancer Res; 22(22); 5564–73.* ©*2016 AACR.*

See related commentary by Janku and Kurzrock, p. 5400

Introduction

In cancer, tumor molecular characterization has become an integral part of diagnostic procedures. In most instances, genomic analyses are performed on tumor tissues obtained from primary tumor or metastatic sites at diagnosis by surgical procedures. Although described for the first time in 1948, it is only recently

[1]INSERM U830, Laboratoire de Génétique et Biologie des Cancers, Research Center, Institut Curie, Paris Sciences et Lettres Research University, Paris, France. [2]Translational Research Department, SiRIC RTOP Recherche Translationelle en Oncologie Pédiatrique, Research Center, Institut Curie, Paris Sciences et Lettres Research University, Paris, France. [3]Plateforme de Génomique des Cancers, Centre Léon Bérard, Lyon, France. [4]Translational Research Department, Genomic Platform, Research Center, Institut Curie, Paris Sciences et Lettres Research University, Paris, France. [5]Unité de Génétique Somatique, Service de Génétique, Hospital Group, Institut Curie, Paris, France. [6]Department of Pediatric Oncology, Hospital Group, Institut Curie, Paris, France. [7]Laboratoire de Recherche Translationnelle, Centre Léon-Bérard, Lyon, France. [8]INSERM U900, Bioinformatics, Biostatistics, Epidemiology and Computational Systems Biology of Cancer, Research Center, Institut Curie, Paris Sciences et Lettres Research University, Paris, France. [9]Institut Curie Genomics of Excellence (ICGex) Platform, Research Center, Institut Curie, Paris, France. [10]Service de Pathologie, Hôpital Robert Debré, APHP and Université Paris Diderot Paris 7, Paris, France. [11]Institut d'Hematologie et d'Oncologie Pédiatrique, Centre Léon Bérard, Lyon, France. [12]Service d'Oncologie Pédiatrique, Hôpital de la Timone, CHU de Marseille, Marseille, France. [13]Service d'Hémato-Oncologie Pédiatrique, CHU Grenoble, Grenoble, France. [14]Service d'Oncologie Pédiatrique, Centre Oscar Lambret, Lille, France. [15]Service d'Hémato-Oncologie Pédiatrique, CHU Nantes, Nantes, France. [16]Unite d'Hemato-Oncologie, Hôpital des Enfants, Toulouse, France. [17]Unité d'onco-hématologie pédiatrique, CHU de Poitiers, Poitiers, France. [18]Department of Pediatric Oncology, Institut Gustave Roussy, Villejuif, France. [19]INSERM UMR-S1052, Centre de Recherche en Cancérologie de Lyon, Lyon, France.

Note: Supplementary data for this article are available at Clinical Cancer Research Online (http://clincancerres.aacrjournals.org/).

V. Combaret and G. Schleiermacher contributed equally to this article.

Corresponding Authors: Gudrun Schleiermacher, Institut Curie, 26 rue d'Ulm, Paris 75248, France. Phone: 3301-4432-4550; Fax: 3301-5310-4005; E-mail: gudrun.schleiermacher@curie.fr; and Valérie Combaret, Laboratoire de Recherche Translationnelle, Centre Léon-Bérard, 28 rue Laennec, Lyon 69373, France. E-mail: valerie.combaret@lyon.unicancer.fr

doi: 10.1158/1078-0432.CCR-16-0500

Translational Relevance

In neuroblastoma, the tumor genomic copy number profile is of prognostic relevance and can determine treatment. However, in rare cases, primary tumor samples are not available. Here, using the OncoScan platform, we demonstrate the feasibility of cell-free DNA (cfDNA) copy number profiling and show that genomic copy number profiles of cfDNA reflect the tumor copy number profile, with a high number of chromosome breakpoints common to tumor aCGH and cfDNA. However, in addition, breakpoints specific to either tumor aCGH or to cfDNA were seen, the latter targeting *IGF1R* and *TERT*, two genes with a role in proliferation and aggressiveness of neuroblastoma, respectively, suggesting the hypothesis that cfDNA might possibly reflect genetic alterations of more aggressive cell clones. These data indicate that cfDNA analysis might be considered a surrogate marker for genomic profiling, enabling sequential analysis, and that these analyses might be of use when exploring the neuroblastoma heterogeneity.

that the study of cell-free nucleic acids has been proposed as a valuable alternative to the study of tumor nucleic acids, indicating that such samples might be considered as surrogate samples for the study of diagnostic, prognostic, and predictive molecular features (1). Many recent studies have demonstrated the feasibility of the study of circulating tumor DNA (ctDNA) in the cell-free DNA (cfDNA) extracted from plasma, or serum, for detecting cancer cell–specific genetic alterations (2–5). These approaches present the advantage of permitting sequential noninvasive sampling.

Neuroblastoma, the most frequent extracranial solid tumor of early childhood, is characterized by a wide variability of its clinical course (6). In addition to clinical, radiologic, and pathologic information, molecular characterization at diagnosis is crucial to determine prognosis and adapt treatment (7). In neuroblastoma, recurrent genetic alterations mainly concern copy number alterations (CNA), whereas genome sequencing studies have revealed an overall low mutation rate of a small number of recurrently altered genes, such as *ALK*, chromatin remodeling or neuritogenesis genes (8–10). Amplification of the *MYCN* oncogene, observed in 20% to 25% of all cases, is associated with a poor prognosis. Other recurrent genetic alterations concern segmental chromosome alterations (SCA) involving more extensive chromosome regions, also associated with a higher risk of relapse, whereas numerical chromosome alterations (NCA) are associated with a good prognosis. Current treatment strategies take into account the genomic copy number profile both in patients with low-risk neuroblastoma, as well as in certain patients with high-risk neuroblastoma, aged <18 months (11, 12). A genomic copy number profile is routinely assessed on diagnostic tumor tissue, most frequently using pangenomic techniques, such as MLPA, array comparative genomic hybridization (aCGH), or SNPa (11, 13, 14). However, in some instances, biopsies from a primary or metastatic tumor site are not available, for instance, in severely ill young infants with disseminated disease, whereas in older children biopsies might harbor only a low percentage of tumor cells, thus impacting on molecular genetic analysis.

Several recent studies have highlighted the importance of both spatial and temporal heterogeneity in neuroblastoma. Indeed, spatial heterogeneity with differences in the genomic profile between different sites or even different clones within a neuroblastoma, or between a primary neuroblastoma and its metastatic sites, have been described, concerning *MYCN*, SCA, or mutations including *ALK* (15, 16). Temporal heterogeneity has been shown to be of importance in neuroblastoma progression, with an accumulation of additional SCA, and clonal evolution with new mutations, such as *ALK* or other MAPK mutations emerging at time of progression (17–19).

The study of cfDNA could represent a potent tool both as a surrogate when primary tumor tissue is not available and for the study of spatial and temporal heterogeneity in neuroblastoma.

Indeed, previous studies have highlighted the feasibility of cfDNA analysis in neuroblastoma, as *MYCN* amplification, chromosome 17q gain, and *ALK* mutations can readily be detected in cfDNA isolated from plasma (2, 20–23). A recent report has suggested that tumor cfDNA might be present in 60% to 70% of neuroblastoma cases at diagnosis (24). However, to date, full genomic profiling on cfDNA has not been performed in neuroblastoma.

The aim of our study was to evaluate the feasibility of genomic copy number profiling of cfDNA isolated from plasma of neuroblastoma patients using the OncoScan platform. We studied a series of 70 cfDNA samples obtained from neuroblastoma patients at diagnosis and compared these with the genomic profile obtained by tumor aCGH.

Materials and Methods

Patients and samples

Patients with neuroblastoma and enrolled in the national multicenter prospective PHRC IC2007-09 biosampling study were included in this study if samples both for genomic copy number profiling of the primary tumor and plasma for genomic copy number profiling of cfDNA obtained at the time of diagnosis were available. A total of 70 patients were included.

Patients were treated in French centers according to the relevant national or international protocols (Supplementary Information). Written informed consent was obtained from parents or guardians according to national law, and ethics approval of protocols was obtained according to national guidelines, and this study was authorized by the ethics committees "Comité de Protection des Personnes Sud-Est IV", references L07–95/L12–171, and "Comité de Protection des Personnes Ile de France", reference 0811728.

aCGH analysis of tumor samples

Following central pathologic review, tumor cell content of samples was determined. After extraction of tumor DNA, genomic copy number analysis was performed by aCGH using NimbleGen or Agilent aCGH platforms. The obtained data were analyzed with NimbleScan or Agilent Workbench softwares, respectively, as described previously (11, 19, 25, 26). *MYCN* copy number status was confirmed by FISH (27).

OncoScan profiling of cfDNA

Plasma samples were obtained at diagnosis by direct venipuncture or more frequently by blood sampling from central venous catheter devices, directly on standard EDTA tubes, and prepared

by centrifugation of blood at 2,000 rpm for 10 minutes, followed by careful aliquoting and freezing at −80°C within 1 to 24 hours after collection. cfDNA was extracted from 200 μL to 1 mL of plasma. Lower volumes (<400 μL) were extracted by centrifugation using the QIAamp DNA Micro Kit, and higher volumes (>400 μL) were extracted using the Qiavac24s system, according to the manufacturer's recommendations (Qiagen). After extraction, cfDNA concentration was measured by Qubit fluorometric assay (Invitrogen). The total cfDNA concentration/mL of plasma was calculated and indicated in ng/mL of plasma. Its quality was defined by analysis on the tape station instrument or bioanalyzer agilent 2100 (Agilent) using the D1000 ScreenTape or High Sensitivity DNA chip, with cfDNA quality expressed as the 200-bp fragment fraction (Supplementary Fig. S1).

The samples were processed for genomic copy number profiling and identification of CNAs through Molecular Inversion Probe (MIP)–based OncoScan Array (Affymetrix). The hybridization, amplification, and labeling protocols were performed according to the manufacturer's recommendations (Affymetrix). Briefly, 20 to 50 ng cfDNA were incubated for annealing of the MIP probe overnight. The annealed DNA was divided in two equal parts and incubated with the gap-fill master mixes AT or GC for ligation. Then the unligated (nongap filled, linear) probes were removed through an exonuclease treatment. The circularized MIP Probes were linearized with a cleavage enzyme, and the first PCR amplification was performed, followed by a second amplification. The amplified products were digested with HaeIII enzyme and hybridized overnight on to the OncoScan Array. The arrays were washed and stained in GeneChip Fluidics Station and scanned in GeneChip Scanner 7G.

The raw data (CEL file) were converted to OSCHP files through OncoScan Console Software (Affymetrix). Data were processed with the SNP-FASST2 segmentation algorithm and analyzed with OncoScan Nexus express for OncoScan 3 software.

In cases with differences between aCGH profiles of the primary neuroblastoma and cfDNA profiles, the origin of samples from the same patient and absence of sample contamination was confirmed using the AuthentiFiler Kit or the AmpFlSTR SGM Plus PCR Amplification Kit (Life Technologies).

Bioinformatics analysis

Genomic copy number profiles obtained by primary tumor aCGH and by cfDNA OncoScan were analyzed.

To perform a comparison of profiles, NimbleGen data had to be converted from hg18 into hg19 reference using UCSC tools LiftOver to match Agilent and OncoScan profiles with hg19 references (28). Normalization of OncoScan data was performed using ChAS-3.0 and OncoScanConsole-1.2 (Affymetrix Software Suite). Then, a circular binary segmentation algorithm was used on both OncoScan and aCGH data (Agilent and NimbleGen) using DNAcopy-1.42.0 (29). Genomic copy number profiles were then generated with DNAcopy-1.42.0, providing visual comparisons.

Breakpoints and chromosome segments with CNAs were then confirmed and annotated using SegAnnDB based on the PrunedDP algorithm (30). A manual correction was additionally applied on the basis of visualization of the profiles.

Common breakpoints were defined as changes in copy number occurring in a window of ±500 kb base pairs, with a change of the same nature (i.e., either a copy number increase or decrease). When comparing chromosome segments identified on tumor aCGH and cfDNA OncoScan copy number profiles, the starting and ending positions of each chromosome segment across all of one sample were equalized using the higher starting and lower ending position of each segment as breakpoint references. All segments across tumor aCGH and cfDNA OncoScan profiles were defined using as reference the smallest segments present at a given position in any of the samples. As OncoScan profiles have a higher resolution than the aCGH platforms used in this study, the number of probes in a given segment could be lower in aCGH as compared with OncoScan profiles. However, the approach used for this analysis ensured that, at a given position, all profiles had the same segment length and that transition between segments represented a breakpoint in at least one of the samples. This enabled comparison between tumor aCGH and OncoScan profiles.

Two measures of similarity between copy number profiles obtained by aCGH of the primary NB and cfDNA analysis were reported (31): (i) the Pearson correlation between tumor aCGH and its respective cfDNA OncoScan copy number profile to compare copy number statuses across all identified CNA segments, given their assumed normal distribution; and (ii) *M*, a measure derived and adapted from the percent concordance (32). *M* is computed as follows, for a (*i,j*) pair.

$$Mi,j = \frac{\#(Si \cap Sj)}{\frac{1}{2} * (\#Si + \#Sj)}$$

Si and *Sj* are the subsets of breakpoints for the OncoScan, *i*, and CGH array, *j*, copy number profile. Similarity between OncoScan and aCGH profiles was determined using the combination of the Pearson correlation and M score reflecting respectively the entire copy number profiles and the localization of breakpoints.

The overall genomic copy number profiles obtained by tumor aCGH or by cfDNA OncoScan analysis were classified according to common criteria. A numerical chromosome alteration (NCA) was defined as probe ratios homogeneously altered throughout entire chromosomes, as compared with the median copy number across the genome. A segmental chromosome alteration (SCA) was defined by the presence of at least 100 contiguous oligonucleotide probes, or covering at least 2 Mb, exhibiting a genomic status different from that of the rest of the chromosome. Breakpoints defining smaller CNAs were not taken into account for the definition of SCA (11, 25, 33). Cases presenting only NCA, without any SCA, were considered as having a "NCA genomic profile." Cases harboring SCA, without or with NCA, were considered as having a "SCA genomic profile." *MYCN* amplification (MNA) was defined as at least three adjacent probes with a fluorescent tumor/normal log2 ratio ≥1.5 and confirmed by FISH on primary tumor tissue and by qPCR in cfDNA (20, 25, 27, 34). In both primary neuroblastoma aCGH and cfDNA OncoScan copy number analysis, a "dynamic" result referred to a copy number profile with at least one CNA, concerning either NCA, or SCA, or MNA. Finally, cases in which no genetic changes were observed were termed "silent" profiles. On the basis of this analysis, presence of ctDNA in the cfDNA sample was inferred in case of presence of CNAs corresponding to CNAs seen in the primary tumor DNA. For estimation of concordance between aCGH and cfDNA genomic profiles, cases with dynamic profiles by both techniques were taken into account. Sensitivity of cfDNA genomic profiling was calculated on the basis of published methods (35).

Results

cfDNA analysis from plasma of neuroblastoma patients

Plasma for cfDNA genomic copy number profiling was available for 70 patients for whom genomic copy number profiling of primary tumor DNA had been performed (stage I or II, $n = 13$; stage III, $n = 11$; stage IV, $n = 39$; stage IVs, $n = 7$; Supplementary Table S1 and Table 1).

Following extraction of cfDNA from plasma, a wide range of cfDNA concentrations was observed (range 15.3–49,700 ng/mL of plasma, mean 1,721 ng/mL, median 323 ng/mL). Higher concentrations of cfDNA were obtained for patients with metastatic versus localized disease (mean 2,528 versus 175 ng/mL of plasma; Mann–Whitney test, $P < 0.000004$; Supplementary Table S1 and Table 1; Fig. 1). A wide range of cfDNA quality as estimated by the 200 bp fraction of the extracted DNA was obtained (200 bp fraction range 2%–98%; mean 63.2%). In 5 cases, the 200 bp fraction was too low to permit calculation (Supplementary Table S1 and Table 1; Supplementary Fig. S1). A significantly higher cfDNA quality was found in patients with metastatic as compared with localized disease (mean 200 bp fraction 70.9% vs. 47%, Mann–Whitney test, $P < 0.002$; Supplementary Table S1).

Comparison of overall copy number profiles between aCGH of the primary neuroblastoma and cfDNA from plasma

Genomic copy number profiles of the primary tumors were classified according to the overall profile. For one patient, aCGH failed. Sixty-two patients showed a dynamic genomic copy number profile. MNA was seen by tumor aCGH in 23 cases: 4 without any other copy number changes, 17 had MNA together with other SCA, and 2 had MNA with only NCA (Supplementary Table S1; Table 1). Among the remaining 39 patients with a dynamic genomic copy number profile, 31 harbored a SCA genomic profile and 8 a NCA genomic profile. Among 7 other patients, the genomic copy number profile did not reveal any copy number changes (silent profile), 4 with localized and 3 with metastatic disease.

Among the 70 cases, cfDNA OncoScan genomic copy number profiling failed in 2 cases due to experimental failure, while results were not interpretable in 2 others (Fig. 2, Table 2).

For the remaining 66 cases, genomic cfDNA copy number profiles were classified according to the same criteria as those used for tumor aCGH (Fig. 2). Fifty-two cases showed a dynamic genomic copy number profile. MNA was seen on the cfDNA OncoScan profile in 22 cases and confirmed by qPCR in cfDNA (20, 34): 2 had an otherwise silent profile, 19 had MNA together with other SCA, and 1 had MNA with only NCA. Thirty other cases had a dynamic copy number profile without MNA, 26 with a SCA, and 4 with a NCA genomic profile. Finally, in 14 other cases, no cfDNA copy number changes could be detected. Among these 14 silent cfDNA OncoScan profiles, all patients but one had localized disease (7 stage I; 3 stage II; 3 stage III; 1 stage IVs).

Among the 62 cases with a dynamic tumor aCGH copy number profile, OncoScan cfDNA analysis concluded the same overall genomic copy number profile in 47 of 62 (75%) cases (Fig. 2). Different results were observed in 15 of 62 cases, 4 due to technical failure of cfDNA analysis, 10 due to silent cfDNA genomic profiles, and only one resulting in a discordant genomic profile (SCA vs. NCA) (Table 2).

Importantly, in 4 of 8 cases with a silent or failed tumor aCGH profile, a dynamic cfDNA profile could be obtained (SCA, $n = 3$; NCA, $n = 1$) (Table 2). Furthermore, for 4 additional cases with an

Table 1. Summary of patients' characteristics, tumor aCGH, and cfDNA OncoScan results according to tumor stage

				cfDNA quantity (ng/mL of plasma)		cfDNA quality (200 bp fraction)		Tumor aCGH genomic profile (number of cases)				cfDNA OncoScan genomic profile (number of cases)			
	N	Age at diagnosis (months), median (range)	*MYCN* amplification (number of cases)	Median	Range	Median	Range	NCA	SCA	MNA	Silent/NI	NCA	SCA	MNA	Silent/NI
Stage I–II	13	29 (4–186)	1	56	15–499	38	2–72	4	4	1	4	0	2	1	10
Stage III	11	19 (1–52)	5	155	15–875	54	15–96	3	3	5	0	2	1	5	3
Stage IV	39	32 (7–160)	14	516	35–49,700	77	16–98	0	22	14	3	0	22	13	4
Stage IVs	7	5 (0.5–10)	3	468	22–3,500	53	15–98	1	2	3	1	2	1	3	1

Abbreviations: MNA, presence of *MYCN* amplification; NCA, genomic profile with NCAs; NI, not interpretable; SCA, genomic profile with the presence of SCAs, without or with NCA.

Table 2. Comparison of overall genomic copy number profiling results by tumor aCGH tumor versus cfDNA OncoScan

cfDNA	aCGH	MNA	SCA genomic profile	NCA genomic profile	Silent profile	Technical failure/no result	Total
MNA		22	0	0	0	0	22
SCA genomic profile		0	22	1	3	0	26
NCA genomic profile		0	0	3	0	1	4
Silent profile		0	6	4	4	0	14
Technical failure/uninterpretable		1	3	0	0	0	4
Total		23	31	8	7	1	70

Abbreviations: MNA, presence of *MYCN* amplification; NCA, genomic profile with NCAs only; SCA, genomic profile with the presence of SCAs, without or with NCA.

aCGH genomic copy number profile without any copy number changes apart from MNA, 3 showed additional SCA on the cfDNA OncoScan profile.

Altogether, based on tumor aCGH as a reference, cfDNA copy number profiling resulted in a sensitivity of 77%. Taking into account cases with dynamic results by both tumor aCGH and cfDNA analysis, the concordance of overall genomic profiles was 97% (47/48 cases: 22 MNAs, 22 SCAs, and 3 NCAs). In only one patient, with localized International Neuroblastoma Staging System (INSS) stage II disease, was an SCA concluded by cfDNA analysis, whereas an NCA genomic profile had been seen by tumor aCGH, the histology of this tumor indicating nodular ganglioneuroblastoma.

When comparing cfDNA OncoScan results according to cfDNA quantity and quality, higher cfDNA quantities were observed in cases with a dynamic profile versus silent profiles (MNA + SCA + NCA vs. silent, mean cfDNA quantity 2,192.87 vs. 104.4 ng/mL, Mann–Whitney test, $P < 0.001$). A higher cfDNA quality was also observed in cases with a dynamic versus a silent OncoScan profile (MNA/SCA/NCA versus silent profiles; 200 bp fraction 69.5% vs. 27%, Mann–Whitney test, $P < 0.001$).

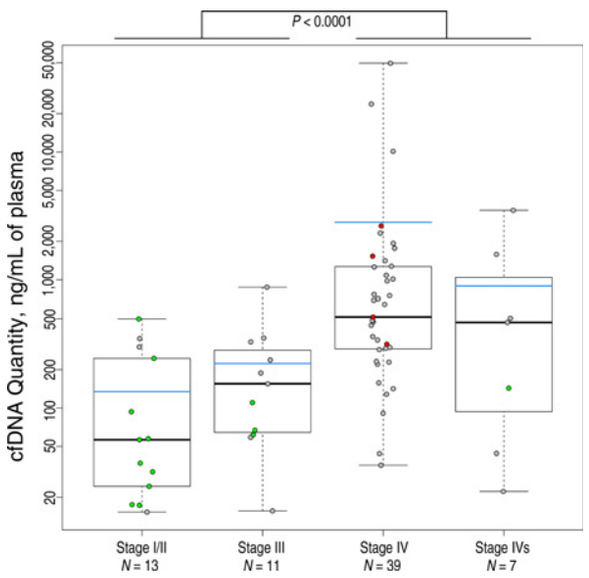

Figure 1.

Correlation between cfDNA quantity and tumor stage. Following extraction of cfDNA from plasma, the cfDNA concentrations per mL of plasma were calculated. The mean cfDNA concentrations (±SE) are indicated according to the INSS stage. cfDNA concentrations were significantly higher in patients with metastatic (stage IV and stage IVs) neuroblastoma as compared with localized (I, II, or stage III) disease ($P < 0.0001$, Mann–Whitney test). Cases for which cfDNA OncoScan failed or resulted in a silent profile are indicated as red or green dots, respectively.

Comparison of breakpoints between aCGH of the primary neuroblastoma and cfDNA from plasma

Chromosome breakpoints observed by aCGH in the primary tumor were compared with those observed by cfDNA analysis from the same patient (Fig. 3). All MNAs seen by aCGH were also seen by cfDNA analysis in the corresponding sample, and vice versa, apart for one case in which cfDNA analysis had failed. To compare breakpoints other than *MYCN* amplification, the 43 cases with dynamic profiles, with copy number changes in addition to *MYCN* amplification both on the aCGH and cfDNA analysis results were then considered in detail.

Large SCAs recurrently observed in neuroblastoma were compared. Among these 43 cases, 109 SCAs were seen both by aCGH and cfDNA analysis, the most frequent being 17q gain ($n = 30$), 1p deletion ($n = 23$), and 11q deletion ($n = 19$).

SCAs detected only by aCGH, but not on an otherwise dynamic cfDNA OncoScan profile, were 1q gain ($n = 2$), 2p gain ($n = 2$), 14q deletion ($n = 1$), and 17q gain ($n = 1$), whereas SCA found only on cfDNA analysis but not on an otherwise dynamic aCGH profile were 1q gain ($n = 1$), 2p gain ($n = 1$), 3p deletion ($n = 2$), 4p deletion ($n = 1$), 14q deletion ($n = 1$), and 17q gain ($n = 1$; Figs. 2 and 3 and Supplementary Fig. S2; Supplementary Table S1). Of note, one case with an overall NCA genomic profile on aCGH showed a large 72 Mb 3p deletion only seen on cfDNA analysis (case 38, Supplementary Fig. S2; Supplementary Table S2).

Taking into account all breakpoints identified among the 43 cases with dynamic profiles both by tumor aCGH and cfDNA analysis ($n = 459$), a total of 378 breakpoints common to both primary neuroblastoma and cfDNA of a given patient were identified, with a mean of 9 breakpoints per case (range 0–30 breakpoints). In addition, 27 breakpoints were only seen by tumor aCGH (mean 0.6 per sample; range 0–4), and 54 breakpoints were seen by cfDNA analysis only (mean 1.3 per sample; range 0–18), highlighting heterogeneity between primary tumor and cfDNA samples (Supplementary Table S2).

To determine the correlation of the breakpoints identified by tumor aCGH and cfDNA analysis, a Pearson correlation score between aCGH and cfDNA data was computed. A mean Pearson correlation score of 0.81 (range 0.1–0.96) was observed (Supplementary Fig. S3). As a further measure of similarity, M as a measure of concordance was analyzed. The mean M score was 0.88 (range 0–1) (Fig. 4). The lowest correlation scores were observed in low-stage disease and in cases of lower cfDNA quality. The highest similarity, defined by the Pearson correlation and M score, thus taking into account the overall genomic copy number profile and the position of the breakpoints, was observed in cases of higher cfDNA quality (Supplementary Table S1).

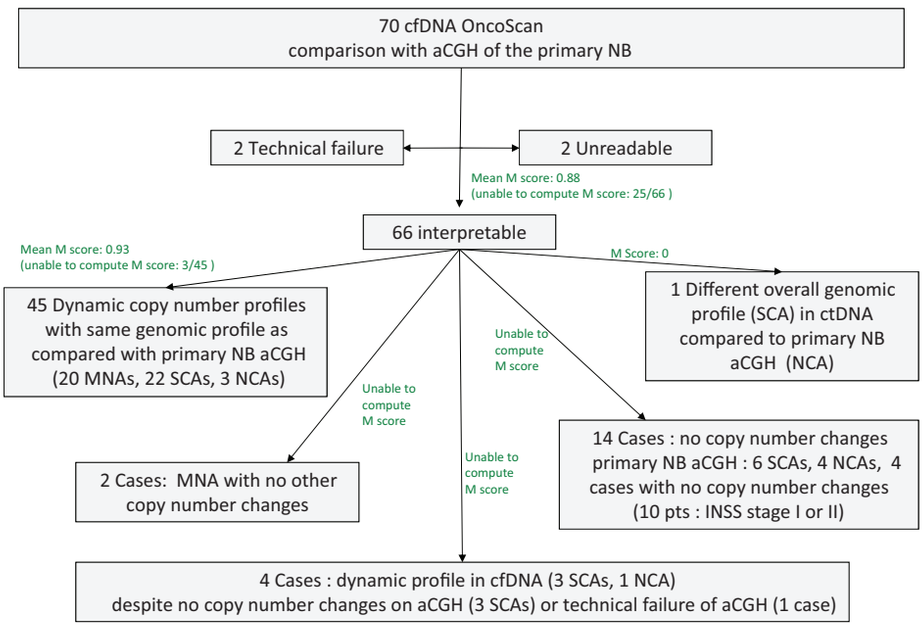

Figure 2.
Summary of results of genomic profiling using cfDNA. NB, neuroblastoma.

We sought to identify breakpoints that might be specific to either primary tumor samples or cfDNA samples. No recurrent breakpoint positions other than those between paired samples were observed. Among breakpoints seen only on primary tumor by aCGH, several breakpoints targeted genes shown previously to play a role in neuroblastoma oncogenesis, such as *PTPRD* (Supplementary Table S2). Among breakpoints seen only on cfDNA by OncoScan, *IGF1R* was targeted by cfDNA breakpoints in 2 separate cases, with a focal amplification encompassing this gene in one, and a high level gain encompassing this gene in a second case (Supplementary Table S2). These CNAs were confirmed by qPCR (Supplementary Fig. S4). Interestingly, *TERT* was targeted by cfDNA-specific breakpoints in 2 cases (Fig. 3D; Supplementary Table S2). The absence of these *TERT*-targeting breakpoints in the corresponding primary neuroblastoma DNA was confirmed by OncoScan (Supplementary Fig. S5).

For one case in which differences between primary neuroblastoma and cfDNA profiles were observed (case 55), the aCGH profile of a bone marrow sample massively invaded by tumor cells, also obtained at diagnosis, could also be performed (Fig. 3D). The cfDNA profile was identical to that of the bone marrow aCGH, showing, in addition to MNA, multiple additional high level gains of chromosome region 5p15.33 to 5p12, harboring, among others, the *GHR*, *EGFLAM*, *PDZD2*, *CHD18*, and *PLEKHG4B* genes, involved in cell growth and signaling pathways. These alterations were not detected on the aCGH of the primary neuroblastoma despite the primary tumor harboring 90% tumor cells.

Altogether, these data clearly demonstrate the feasibility of genomic copy number profiling of cfDNA obtained from plasma at diagnosis from neuroblastoma patients.

Discussion

The study of nucleic acids isolated from plasma has been proposed only recently for the characterization of cancer cell–derived genomic alterations, including the study of DNA, mRNA, miRNA, and epigenetic markers (2, 20–24, 36–38). CfDNA is thought to be related to the apoptosis and necrosis of cancer cells, with fragments of cellular nucleic acids either being actively released or following phagocytosis and subsequent release by macrophages and other scavenger cells. The usefulness of cfDNA as surrogate liquid biopsies for biomarkers is now being widely explored.

In neuroblastoma, it has been shown that the overall tumor genomic profile determined by copy number analysis of tumor material is of prognostic impact, and genomic copy number profiling using material from tumor cells is considered as a reference for obtaining a tumor genomic profile at the time of diagnosis (11, 13, 14). We have now undertaken a study of 70 plasma samples obtained at diagnosis to determine the feasibility of using cfDNA isolated from plasma for the study of an overall genomic profile.

In neuroblastoma, several studies have clearly documented the presence of cfDNA in particular in patients with metastatic disease (2, 20–24, 34, 39). In the current study, although no precise information regarding overall tumor load (primary tumor volume; number, and size of metastatic sites) was available, higher concentrations of cfDNA were observed for patients with metastatic as compared with localized disease. The feasibility of genomic copy number profiling using cfDNA obtained from neuroblastoma patients at diagnosis could be demonstrated, with technical success of cfDNA OncoScan analysis in 66 of 70 (94%) cases and dynamic genomic profiles obtained in 52 of 70 (74%) of all cases. CfDNA analysis provided informative results in 48 of 62 (77.4%) cases with dynamic and in 4 of 8 (50%) cases with silent or failed tumor aCGH results. In cases with dynamic copy number profiles by both aCGH and cfDNA analysis, an excellent concordance of 97% between the overall copy number profiles was observed.

On the other hand, silent cfDNA profiles were obtained in 14 of 70 (20%) of all cases, 10 of which had dynamic aCGH results,

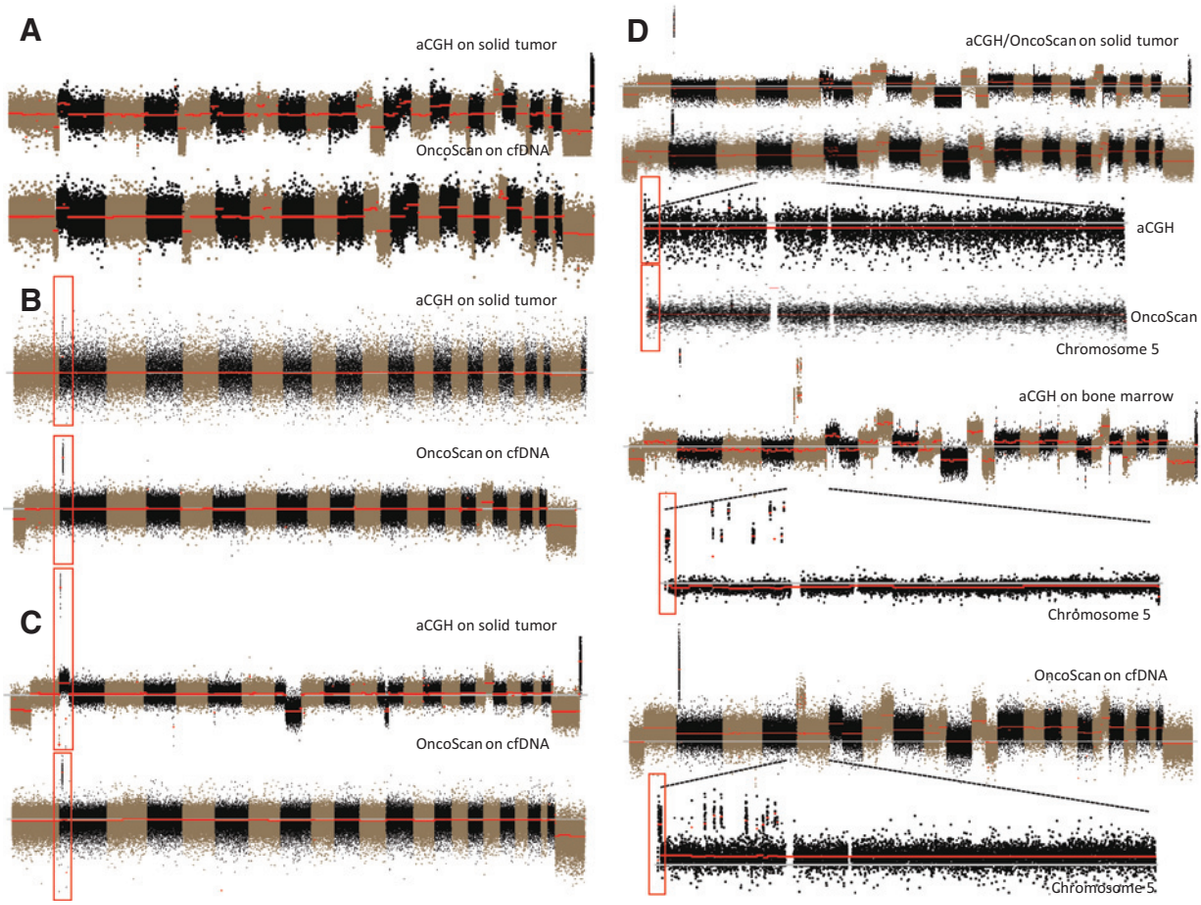

Figure 3.

Comparison of copy number profiles of neuroblastoma samples compared to cfDNA. **A,** identical profile between aCGH of primary neuroblastoma and OncoScan of cfDNA, showing, among others, chromosome 2p, 12q, and 17q gain, as well as chromosome 1q, 5p, and 11q loss (case number 62, stage IV). **B,** silent profile on tumor aCGH of primary neuroblastoma, apart from MNA, and dynamic profile on cfDNA OncoScan revealing MNA and several SCAs (loss of chr 1p and gain of chr 17q; case number 27, stage III). The *MYCN* locus is boxed in red. **C,** aCGH of primary neuroblastoma showing SCA and *MYCN* amplification, OncoScan of cfDNA showing *MYCN* amplification (case number 51, stage IIb). The *MYCN* locus is boxed in red. **D,** comparison of genomic copy number profiles of primary neuroblastoma (studied by aCGH and OncoScan), and bone marrow metastasis (studied by aCGH), compared with cfDNA (studied by OncoScan). The profiles of the primary tumor and the bone marrow metastasis harbor MNA, 1p deletion, 7q gain, 11q deletion, and 17 q gain. In addition, the bone marrow metastasis shows several high level gains on chr 5p. cfDNA analysis revealed a profile identical to that of the bone marrow, with one breakpoint targeting *TERT* seen only in the bone marrow and the cfDNA but not the primary neuroblastoma, and high level gains harboring, among others, the *GHR, EGFLAM, PDZD2, CHD18*, and *PLEKHG4B* genes (case number 55). The *TERT* locus is boxed in red.

resulting in a false negative rate of 10/62 (16.1%). Silent cfDNA profiles were observed more frequently in INSS stage I or II (10/13 patients) and in cases of lower cfDNA quality and quantity. This is consistent with previous studies (24, 34) and further suggests that in patients with low-risk disease, fewer cfDNA-releasing cells were present.

Differences in genomic copy number profiles observed between primary neuroblastoma aCGH and cfDNA OncoScan analysis might be due to either technical issues or tumor heterogeneity.

Technical issues might involve low tumor cell content in the studied sample: tumor cell content below 20% to 30% in the primary neuroblastoma sample results in a silent copy number profile by aCGH (11), and likewise a silent OncoScan profile is expected if the ctDNA fraction is below this cutoff in the cfDNA sample.

Among the 19 of 70 cases in which primary aCGH and cfDNA OncoScan analysis concluded a different overall genomic copy number result, 5 were due to technical failure (1 by aCGH, 4 by cfDNA OncoScan analysis), 10 were due to a silent cfDNA profile, and 3 due to a silent aCGH profile.

Tumor heterogeneity might also account for the observed differences. In neuroblastoma, both spatial and temporal heterogeneity have been described. Spatial heterogeneity might concern genomic heterogeneity between a primary tumor and its metastatic sites, between different tumor nodules or components within a single primary, or even between different tumor (sub) clones and has been described for *MYCN* or *ALK* genomic status (15–18, 23, 40). As cfDNA might reflect preferentially genomic alterations linked to specific cellular characteristics with different dynamics of proliferation, necrosis, or apoptosis, the comparison

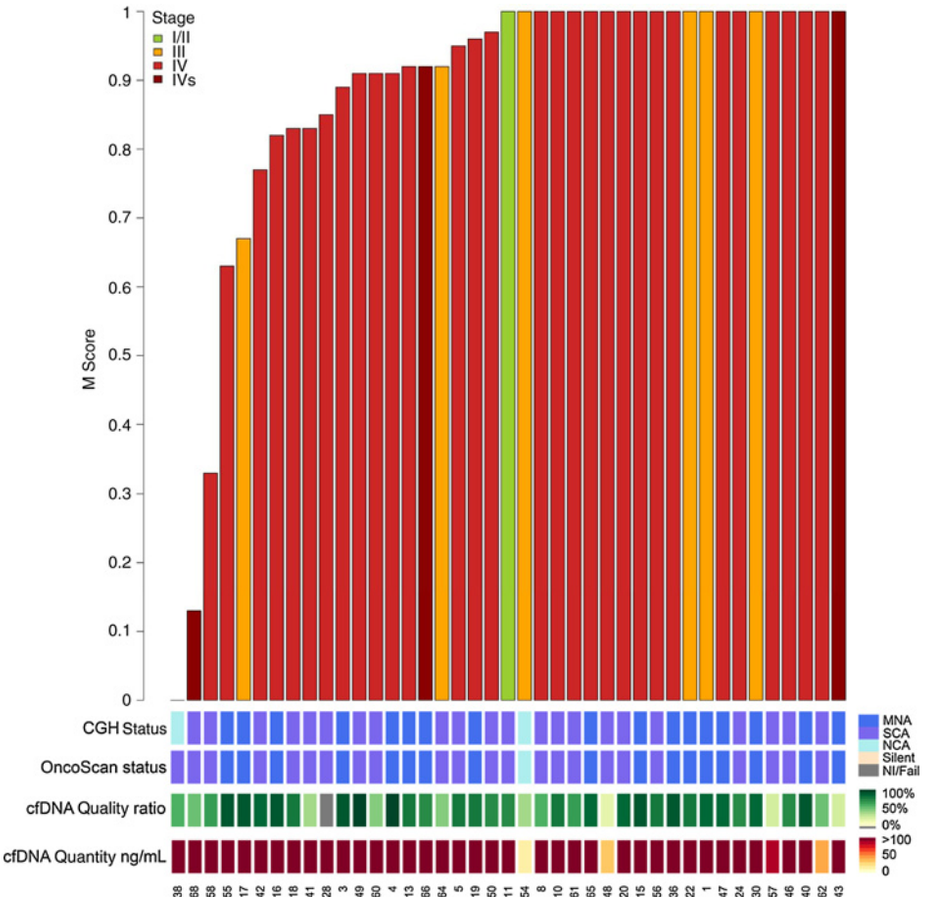

Figure 4.
Correlation of genomic profiles determined by tumor aCGH and cfDNA analysis. The M score, comparing the presence of breakpoints in all cases harboring SCA genomic profiles, is indicated. Tumor stage is indicated according to a color code of the correlation bars. Bottom, results of aCGH and cfDNA analysis and cfDNA quality and quantity.

of cfDNA to tumor aGCH is crucial to further determine this potential heterogeneity.

Despite a high number of chromosome breakpoints identified in both the primary neuroblastoma by aCGH and the corresponding cfDNA (378/459, 82.4%), detailed comparison of chromosome breakpoints observed by either technique revealed differences with some breakpoints seen only in the primary neuroblastoma and others only in cfDNA.

Differences of breakpoints detected in the primary neuroblastoma and the corresponding cfDNA might possibly be explained by technical bias due to the difference of coverage between aCGH and OncoScan platforms, the latter providing a denser coverage over cancer genes. Nevertheless, the bioinformatics analysis employed in this study aimed at equalizing segments at a given position across different platforms, thus correcting for potential coverage-related bias. Thus, the observation of breakpoints seen only in the primary neuroblastoma and not the cfDNA (27/459, 5.9%) suggests that these alterations detected only in a biopsy of the primary neuroblastoma might concern tumor cells that show less necrosis/apoptosis, perhaps a lower cell turnover, and thus are less at the origin of release of cfDNA.

On the other hand, the observation that some breakpoints are only seen in cfDNA and not in aCGH of the primary neuroblastoma (54/459, 11.8%) indicates that genetic alterations observed in cfDNA-releasing cells are not common to all tumor cells of a given patient. Indeed, these cfDNA-specific breakpoints occurred in patients for whom primary neuroblastoma aCGH had resulted in a dynamic copy number result, and thus a detection failure of these apparently cfDNA-specific breakpoints due to low tumor cell content of the primary neuroblastoma sample is highly unlikely. The breakpoint-containing cfDNA might correspond to primary neuroblastoma cells from areas not accessed and sampled by biopsy, or present in a subclone only, below detection limit of aCGH analysis. The cfDNA might also correspond to cells from metastatic sites. The observation of a cfDNA profile distinct from its primary neuroblastoma but identical to that of a strongly invaded bone marrow favors such a hypothesis. Furthermore, in patients with clinically localized disease and cfDNA-specific breakpoints, it cannot be excluded that micrometastasis not detected by routine clinical examination might have contributed to the alterations seen in the cfDNA profile.

When searching for recurrent CNAs specific to cfDNA, focal high level *IGF1R* gains were observed in cfDNA of 2 patients. Indeed, IGF1R signaling, which plays an important role in cancer cell proliferation, has been shown to play a role in the neuroblastoma malignant phenotype (41–44). Furthermore, in 2 cases, an alteration targeting *TERT*, shown recently to characterize aggressive high-risk neuroblastoma (45, 46), was identified in the cfDNA, with one case harboring this alteration also in the metastatic tumor cells of the bone marrow but not in the primary neuroblastoma. It might be hypothesized that these genetic alterations, both associated with tumor proliferation and a more

malignant phenotype, were found in the cfDNA due to their presence in cells more prone to cfDNA release, which might be cells with a stronger cell growth and higher aggressiveness.

Overall, both patients with localized and metastatic disease harbored cfDNA-specific breakpoints, suggesting that spatial heterogeneity both within a large primary neuroblastoma and between a primary neuroblastoma and its metastases can occur. Further studies of multiple biopsies and comparison with metastatic tumor sites will help to determine whether alterations observed in cfDNA do indeed represent alterations from cells more readily prone to necrosis or apoptosis and release of cfDNA and might also reveal whether such cell clones are located homogeneously throughout one neuroblastoma, or whether there might be more distinct spatial heterogeneity.

In addition to spatial heterogeneity, temporal heterogeneity has recently been shown to be of importance in neuroblastoma progression (17, 18). However, in most solid tumors, multiple sequential biopsies are not feasible, underlining the urgent need to identify surrogate biological samples for sequential biomarker analysis.

The usefulness of cfDNA analysis for the documentation of tumor heterogeneity has been recently been widely documented, focusing mainly on studies of mutations using next-generation sequencing approaches (1, 38, 47). Several recent studies have also demonstrated the feasibility and usefulness of the detection of tumor-specific CNAs in cfDNA from cancer patients. Shotgun massively parallel sequencing of cfDNA was used to achieve genome-wide copy number profiling in hepatocellular carcinoma patients (48). Copy number profiling of cfDNA could also be achieved following whole-genome amplification and aCGH on a microarray platform in colorectal and breast cancer patients (49).

In this study, the commercialized OncoScan platform was used, designed specifically for analyzing small fragmented DNA molecules, and requiring little cfDNA input (minimum 20 ng of cfDNA), permitting a rapid analysis of the cfDNA copy number profile in a readily accessible setting.

In conclusion, we now demonstrate the feasibility of tumor genomic copy number profiling of cfDNA in neuroblastoma patients at diagnosis. Such cfDNA analyses should not replace routine molecular diagnostic techniques but might provide important information in cases where routine molecular characterization of tumor tissue cannot be performed, for instance, in samples with poor tumor cell content, poor DNA quality, or in very sick neuroblastoma patients for whom no tumor biopsy can be performed. In particular, this approach might be of interest in the context of treatment protocols that take into account a tumor genomic profile for therapeutic stratification, such as the European Low and Intermediate Risk Neuroblastoma Protocol LINES protocol (ClinicalTrials.gov identifier NCT01728155; ref. 50). Future prospective studies will be necessary to determine the feasibility and success rate of cfDNA genomic profiling in particular in low-risk neuroblastoma patients, or high-risk neuroblastoma patients aged <18 months, where genomic profile might determine treatment, and to establish clearly for which patients such an analysis might serve as surrogate if a representative tumor sample cannot be obtained. Furthermore, given the importance of spatial and temporal heterogeneity in neuroblastoma, such cfDNA copy number analysis might enable further studies of both diagnostic and subsequent relapse CNAs in neuroblastoma patients, which might reflect genetic alterations of more aggressive or metastatic cell clones. We suggest that collection of plasma for cfDNA studies could constitute a component of ancillary studies of early clinical trials to enable the study of tumor heterogeneity and evolution of genomic copy number changes during treatment.

Disclosure of Potential Conflicts of Interest

No potential conflicts of interest were disclosed.

Authors' Contributions

Conception and design: M. Chicard, D. Gentien, A. Puisieux, O. Delattre, V. Combaret, G. Schleiermacher

Development of methodology: M. Chicard, D. Gentien, G. Schleiermacher

Acquisition of data (acquired and managed patients, provided facilities, etc.): M. Chicard, S. Boyault, D. Gentien, G. Pierron, E. Lapouble, N. Clement, I. Iacono, S. Bréjon, C. Reyes, M. Peuchmaur, C. Faure-Conter, C. Coze, D. Plantaz, A.S. Defachelles, E. Thebaud, M. Gambart, F. Millot, J. Michon, O. Delattre, G. Schleiermacher

Analysis and interpretation of data (e.g., statistical analysis, biostatistics, computational analysis): M. Chicard, L. Colmet Daage, W. Richer, T. Hocking, V. Bernard, M. Peuchmaur, V. Combaret, G. Schleiermacher

Writing, review, and/or revision of the manuscript: M. Chicard, L. Colmet Daage, W. Richer, E. Lapouble, V. Bernard, M. Peuchmaur, N. Corradini, C. Coze, D. Plantaz, E. Thebaud, D. Valteau-Couanet, A. Puisieux, O. Delattre, V. Combaret, G. Schleiermacher

Administrative, technical, or material support (i.e., reporting or organizing data, constructing databases): M. Chicard, D. Gentien, G. Pierron, A. Bellini, N. Clement, I. Iacono, S. Bréjon, M. Carrere, C. Reyes, D. Plantaz, D. Valteau-Couanet, O. Delattre, V. Combaret, G. Schleiermacher

Study supervision: M. Chicard, V. Combaret, G. Schleiermacher

Acknowledgments

The authors thank the clinicians and pathologists of the SFCE (Société Française de Lutte contre les Cancers et Leucémies de l'Enfant et de l'Adolescent).

Grant Support

This study was supported by the Annenberg Foundation, the Nelia and Amadeo Barletta Foundation (FNAB), and the Association Hubert Gouin Enfance et Cancer. This study was also funded by the Associations Enfants et Santé, Les Bagouz à Manon, and Les amis de Claire. Funding was also obtained from SiRIC/INCa (grant INCa-DGOS-4654), LYRIC/INCA (grant INCa-DGOS-4664), the CEST of Institute Curie, and PHRCIC2007-09 grant.

The costs of publication of this article were defrayed in part by the payment of page charges. This article must therefore be hereby marked *advertisement* in accordance with 18 U.S.C. Section 1734 solely to indicate this fact.

Received February 24, 2016; revised June 4, 2016; accepted June 28, 2016; published OnlineFirst July 20, 2016.

References

1. Schwarzenbach H, Hoon DS, Pantel K. Cell-free nucleic acids as biomarkers in cancer patients. Nat Rev Cancer 2011;11:426–37.
2. Combaret V, Audoynaud C, Iacono I, Favrot MC, Schell M, Bergeron C, et al. Circulating *MYCN* DNA as a tumor-specific marker in neuroblastoma patients. Cancer Res 2002;62:3646–8.
3. De Mattos-Arruda L, Caldas C. Cell-free circulating tumour DNA as a liquid biopsy in breast cancer. Mol Oncol 2016;10:464–74.
4. Huang SK, Hoon DS. Liquid biopsy utility for the surveillance of cutaneous malignant melanoma patients. Mol Oncol 2016;10:450–63.

5. Jovelet C, Ileana E, Le Deley MC, Motté N, Rosellini S, Romero A, et al. Circulating cell-free tumor DNA(cfDNA) analysis of 50-genes by next-generation sequencing (NGS) in the prospective MOSCATO trial. Clin Cancer Res 2016;22:2960–8.
6. Maris JM, Hogarty MD, Bagatell R, Cohn SL. Neuroblastoma. Lancet 2007; 369:2106–20.
7. Schleiermacher G, Janoueix-Lerosey I, Delattre O. Recent insights into the biology of neuroblastoma. Int J Cancer 2014;135:2249–61.
8. Molenaar JJ, Koster J, Zwijnenburg DA, van Sluis P, Valentijn LJ, van der Ploeg I, et al. Sequencing of neuroblastoma identifies chromothripsis and defects in neuritogenesis genes. Nature 2012;483:589–93.
9. Pugh TJ, Morozova O, Attiyeh EF, Asgharzadeh S, Wei JS, Auclair D, et al. The genetic landscape of high-risk neuroblastoma. Nat Genet 2013;45:279–84.
10. Sausen M, Leary RJ, Jones S, Wu J, Reynolds CP, Liu X, et al. Integrated genomic analyses identify *ARID1A* and *ARID1B* alterations in the childhood cancer neuroblastoma. Nat Genet 2013;45:12–7.
11. Janoueix-Lerosey I, Schleiermacher G, Michels E, Mosseri V, Ribeiro A, Lequin D, et al. Overall genomic pattern is a predictor of outcome in neuroblastoma. J Clin Oncol 2009;27:1026–33.
12. Cohn SL, Pearson AD, London WB, Monclair T, Ambros PF, Brodeur GM, et al. The International Neuroblastoma Risk Group (INRG) classification system: an INRG Task Force report. J Clin Oncol 2009;27:289–97.
13. Ambros IM, Brunner B, Aigner G, Bedwell C, Beiske K, Bénard J, et al. A multilocus technique for risk evaluation of patients with neuroblastoma. Clin Cancer Res 2011;17:792–804.
14. Ambros IM, Brunner C, Abbasi R, Frech C, Ambros PF. Ultra-high density SNParray in neuroblastoma molecular diagnostics. Front Oncol 2014; 4:202.
15. Theissen J, Boensch M, Spitz R, Betts D, Stegmaier S, Christiansen H, et al. Heterogeneity of the *MYCN* oncogene in neuroblastoma. Clin Cancer Res 2009;15:2085–90.
16. Bellini A, Bernard V, Leroy Q, Rio Frio T, Pierron G, Combaret V, et al. Deep sequencing reveals occurrence of subclonal *ALK* mutations in neuroblastoma at diagnosis. Clin Cancer Res 2015;21:4913–21.
17. Schramm A, Koster J, Assenov Y, Althoff K, Peifer M, Mahlow E, et al. Mutational dynamics between primary and relapse neuroblastomas. Nat Genet 2015;47:872–7.
18. Eleveld TF, Oldridge DA, Bernard V, Koster J, Daage LC, Diskin SJ, et al. Relapsed neuroblastomas show frequent *RAS-MAPK* pathway mutations. Nat Genet 2015;47:864–71.
19. Schleiermacher G, Janoueix-Lerosey I, Ribeiro A, Klijanienko J, Couturier J, Pierron G, et al. Accumulation of segmental alterations determines progression in neuroblastoma. J Clin Oncol 2010;28:3122–30.
20. Combaret V, Bergeron C, Noguera R, Iacono I, Puisieux A. Circulating *MYCN* DNA predicts *MYCN*-amplification in neuroblastoma. J Clin Oncol 2005;23:8919–20.
21. Gotoh T, Hosoi H, Iehara T, Kuwahara Y, Osone S, Tsuchiya K, et al. Prediction of *MYCN* amplification in neuroblastoma using serum DNA and real-time quantitative polymerase chain reaction. J Clin Oncol 2005;23:5205–10.
22. Combaret V, Brejon S, Iacono I, Schleiermacher G, Pierron G, Ribeiro A, et al. Determination of 17q gain in patients with neuroblastoma by analysis of circulating DNA. Pediatr Blood Cancer 2011;56:757–61.
23. Combaret V, Iacono I, Bellini A, Bréjon S, Bernard V, Marabelle A, et al. Detection of tumor *ALK* status in neuroblastoma patients using peripheral blood. Cancer Med 2015;4:540–50.
24. Bettegowda C, Sausen M, Leary RJ, Kinde I, Wang Y, Agrawal N, et al. Detection of circulating tumor DNA in early- and late-stage human malignancies. Sci Transl Med 2014;6:224ra24.
25. Guimier A, Ferrand S, Pierron G, Couturier J, Janoueix-Lerosey I, Combaret V, et al. Clinical characteristics and outcome of patients with neuroblastoma presenting genomic amplification of loci other than *MYCN*. PLoS One 2014;9:e101990.
26. Combaret V, Iacono I, Brejon S, Schleiermacher G, Pierron G, Couturier J, et al. Analysis of genomic alterations in neuroblastoma by multiplex ligation-dependent probe amplification and array comparative genomic hybridization: a comparison of results. Cancer Genet 2012;205:657–64.
27. Ambros PF, Ambros IM, Brodeur GM, Haber M, Khan J, Nakagawara A, et al. International consensus for neuroblastoma molecular diagnostics: report from the International Neuroblastoma Risk Group (INRG) Biology Committee. Br J Cancer 2009;100:1471–82.
28. Kent WJ, Sugnet CW, Furey TS, Roskin KM, Pringle TH, Zahler AM, et al. The human genome browser at UCSC. Genome Res 2002;12:996–1006.
29. Seshan V, Olshen A. DNAcopy: DNA copy number data analysis. R package version 1.46.0; 2016. Available from: http://bioconductor.org/packages/DNAcopy/.
30. Hocking TD, Boeva V, Rigaill G, Schleiermacher G, Janoueix-Lerosey I, Delattre O, et al. SegAnnDB: interactive web-based genomic segmentation. Bioinformatics 2014;30:1539–46.
31. Bollet MA, Servant N, Neuvial P, Decraene C, Lebigot I, Meyniel JP, et al. High-resolution mapping of DNA breakpoints to define true recurrences among ipsilateral breast cancers. J Natl Cancer Inst 2008;100:48–58.
32. Waldman FM, DeVries S, Chew KL, Moore DHII, Kerlikowske K, Ljung BM. Chromosomal alterations in ductal carcinomas *in situ* and their *in situ* recurrences. J Natl Cancer Inst 2000;92:313–20.
33. Schleiermacher G, Mosseri V, London WB, Maris JM, Brodeur GM, Attiyeh E, et al. Segmental chromosomal alterations have prognostic impact in neuroblastoma: a report from the INRG project. Br J Cancer 2012;107: 1418–22.
34. Combaret V, Hogarty MD, London WB, McGrady P, Iacono I, Brejon S, et al. Influence of neuroblastoma stage on serum-based detection of *MYCN* amplification. Pediatr Blood Cancer 2009;53:329–31.
35. Delacour H, Servonnet A, Perrot A, Vigezzi JF, Ramirez JM. [ROC (receiver operating characteristics) curve: principles and application in biology]. Ann Biol Clin 2005;63:145–54.
36. Stroun M, Maurice P, Vasioukhin V, Lyautey J, Lederrey C, Lefort F, et al. The origin and mechanism of circulating DNA. Ann N Y Acad Sci 2000; 906:161–8.
37. Diaz LAJr, Bardelli A. Liquid biopsies: genotyping circulating tumor DNA. J Clin Oncol 2014;32:579–86.
38. Haber DA, Velculescu VE. Blood-based analyses of cancer: circulating tumor cells and circulating tumor DNA. Cancer Discov 2014;4:650–61.
39. Kurihara S, Ueda Y, Onitake Y, Sueda T, Ohta E, Morihara N, et al. Circulating free DNA as non-invasive diagnostic biomarker for childhood solid tumors. J Pediatr Surg 2015;50:2094–7.
40. Schleiermacher G, Javanmardi N, Bernard V, Leroy Q, Cappo J, Rio Frio T, et al. Emergence of new *ALK* mutations at relapse of neuroblastoma. J Clin Oncol 2014;32:2727–34.
41. Wojtalla A, Salm F, Christiansen DG, Cremona T, Cwiek P, Shalaby T, et al. Novel agents targeting the *IGF-1R/PI3K* pathway impair cell proliferation and survival in subsets of medulloblastoma and neuroblastoma. PLoS One 2012;7:e47109.
42. DeNardo BD, Holloway MP, Ji Q, Nguyen KT, Cheng Y, Valentine MB, et al. Quantitative phosphoproteomic analysis identifies activation of the *RET* and *IGF-1R/IR* signaling pathways in neuroblastoma. PLoS One 2013;8: e82513.
43. Ho WL, Chou CH, Jeng YM, Lu MY, Yang YL, Jou ST, et al. GALNT2 suppresses malignant phenotypes through IGF-1 receptor and predicts favorable prognosis in neuroblastoma. Oncotarget 2014;5: 12247–59.
44. Qi L, Toyoda H, Shankar V, Sakurai N, Amano K, Kihira K, et al. Heterogeneity of neuroblastoma cell lines in *insulin-like growth factor 1 receptor/Akt* pathway-mediated cell proliferative responses. Cancer Sci 2013;104: 1162–71.
45. Valentijn LJ, Koster J, Zwijnenburg DA, Hasselt NE, van Sluis P, Volckmann R, et al. *TERT* rearrangements are frequent in neuroblastoma and identify aggressive tumors. Nat Genet 2015;47:1411–4.
46. Peifer M, Hertwig F, Roels F, Dreidax D, Gartlgruber M, Menon R, et al. Telomerase activation by genomic rearrangements in high-risk neuroblastoma. Nature 2015;526:700–4.
47. Newman AM, Bratman SV, To J, Wynne JF, Eclov NC, Modlin LA, et al. An ultrasensitive method for quantitating circulating tumor DNA with broad patient coverage. Nat Med 2014;20:548–54.
48. Chan KC, Jiang P, Zheng YW, Liao GJ, Sun H, Wong J, et al. Cancer genome scanning in plasma: detection of tumor-associated copy number aberrations, single-nucleotide variants, and tumoral heterogeneity by massively parallel sequencing. Clin Chem 2013;59:211–24.
49. Heitzer E, Auer M, Hoffmann EM, Pichler M, Gasch C, Ulz P, et al. Establishment of tumor-specific copy number alterations from plasma DNA of patients with cancer. Int J Cancer 2013;133:346–56.
50. National Institutes of Health. ClinicalTrials.gov. 2016. Available from: https://clinicaltrials.gov/ct2/show/NCT01728155.